Toward a Single-Valued DMBE Potential Energy Surface for CHNO(^{3}A). 1. Diatomic Fragments

P. Jimeno and J. C. Rayez*

Laboratoire de Physicochimie Théorique, CNRS URA 503, Université Bordeaux 1, 351 Cours de la Libération 33405, Talence, France

P. E. Abreu and A. J. C. Varandas*

Departamento de Química, Universidade de Coimbra, P-3049 Coimbra Codex, Portugal

Received: February 26, 1997[⊗]

As a first step toward the construction of a single-valued double many-body expansion potential energy surface for CHNO(^{3}A), we have carried out CASSCF and CASPT2 calculations of six diatomic curves, involving a total of nine electronic states. The *ab initio* curves have been represented analytically using the extended Hartree−Fock approximate correlation energy model. In all cases, the semiempirical curves have been found to agree well with the available spectroscopic RKR data.

1. Introduction

To accurately describe the dynamics of chemical reactions, it is essential to have a good global representation of the involved potential energy surface (PES) or surfaces. In this way, the treatment of a tetraatomic system such as CHNO becomes a formidable task since we deal with a six-dimensional PES. In addition, all fragments which are allowed by the spin-spatial correlation rules must be taken into account to achieve a realistic description of the PES in the asymptotic reactive channels. To represent such a global PES, many analytical approaches have been proposed in the literature.[1−6] Among them, the double many-body expansion[4,7,8] (DMBE) method offers one of the most intuitive approaches, which has been successfully applied to triatomic[4,9−12] and tetraatomic[13−15] systems. Moreover, it has the great advantage of assuming the proper functional dependence on the interatomic separation of the long-range interactions, which has been shown to play an important role both in reactive and nonreactive collisions.

In the DMBE method, the molecular potential energy for a *N*-atom system is written as a sum of terms, each dealing with a cluster of *n* atoms (from one to *N*), in turn partitioned into extended Hartree−Fock (EHF) and dynamical correlation (dc) parts,

$$V(R^N) = \sum_{n=1}^{N} \sum_{R^n \subset R^N} [V_{\mathrm{EHF}}^{(n)}(R^n) + V_{\mathrm{dc}}^{(n)}(R^n)] \qquad (1)$$

where R^n denotes any set of $[n(n-1)/2]$ coordinates referring to *n* atoms, which is a subset of $R^N \equiv [R_1, R_2, ..., R_{N(N-1)/1}]$, and the last sum in eq 1 is carried out over all such subsets. Accordingly, $V^{(n)}$ must vanish if any of the *n* atoms in the cluster is removed from the rest of the *n*-atom subsystem. In order to apply the DMBE method to the CHNO(^{3}A) PES, it is therefore necessary to describe all the diatomic, triatomic, and tetratomic fragments which correlate with the relevant electronic state of the tetraatomic by the Wigner−Witmer rules. These fragments are listed in Table 1.

The aim of the present work is to provide a reliable description of the diatomic fragments in Table 1. This involves a comparison of the results obtained using five different basis sets in order to reach a reasonable description of the diatomics at an acceptable computational cost since, for consistency, the same level of sophistication should be kept in the calculations referring to the triatomic and tetratomic fragments. In this work we present also analytical fits of the calculated energies for both the extended Hartree−Fock and the dynamical correlation; the former has been estimated from CASSCF calculations, while the latter has been calculated using the CASPT2[16] method with the CASSCF wave function as reference.

The plan of the paper is as follows. Section 2 describes briefly the model, while the computational and technical details are given in section 3. In section 4, we present and analyse the results obtained. The conclusions are in section 5.

TABLE 1: Wigner−Witmer Correlation Rules for CHNO(^{3}A) and Associated Fragments

HCNO(^{3}A)	→	HCN(^{1}A′) + O(^{3}P)
	→	HNO(^{1}A′) + C(^{3}P)
	→	CNO(^{2}A′) + H(^{2}S)
	→	HCO(^{2}A′) + N(^{4}S)
	→	HC($X^2\Pi$) + NO($X^2\Pi$) HC($a^4\Sigma^-$) + NO($X^2\Pi$)
	→	HN($X^3\Sigma^-$) + CO($X^1\Sigma$)
	→	HO($X^2\Pi$) + CN($X^2\Sigma$) HO($a^4\Sigma^-$) + CN($X^2\Sigma$)
	→	H(^{2}S) + C(^{3}P) + N(^{4}S) + O(^{3}P)
HCN(^{1}A′)	→	CN($X^2\Sigma$) + H(^{2}S)
	→	NH($X^3\Sigma^-$) + C(^{3}P)
	→	HC($a^4\Sigma^-$) + N(^{4}S)
HNO(^{1}A′)	→	NO($X^2\Pi$) + H(^{2}S)
	→	HO($X^2\Pi$) + N(^{2}D) HO($a^4\Sigma^-$) + N(^{4}S)
	→	NH($X^3\Sigma^-$) + O(^{3}P)
CNO(^{2}A′)	→	NO($X^2\Pi$) + C(^{3}P)
	→	CN($X^2\Sigma$) + H(^{2}S)
	→	CO($X^1\Sigma$) + N(^{2}D) CO($a^3\Pi$) + N(^{4}S)
HCO(^{2}A′)	→	HO($X^2\Pi$) + C(^{3}P)
	→	HC($X^2\Pi$) + O(^{3}P)
	→	CO($X^1\Sigma$) + H(^{2}S)

2. Method

If we restrict ourselves to the diatomic molecules in Table 1, eq 1 becomes

[⊗] Abstract published in *Advance ACS Abstracts,* June 1, 1997.

S1089-5639(97)00720-2 CCC: $14.00

$$V^{(2)} = V^{(2)}_{\mathrm{EHF}}(R) + V^{(2)}_{\mathrm{dc}}(R) \tag{2}$$

where V_{EHF} represents the extended Hartree−Fock energy and V_{dc} is the dynamical correlation term which includes the asymptotic long range dispersion energy; since we deal only with the diatomic fragments, we will drop for simplicity in the following the superscript (2). Thus, the model is commonly referred to by the acronym EHFACE2, after the initials of extended hartree−fock approximate correlation energy (the digital stands for diatomics); for an extension of this model which includes the proper united atom limit behavior and incorporates the asymptotic exchange energy, the reader is refered to ref 17.

As usual[4] we now represent the EHF part of the potential energy curve by the form

$$V_{\mathrm{EHF}} = -DR^{-1}(1 + \sum_{i=1}^{3} a_i r^i)\, e^{-\gamma r} \tag{3}$$

where $r = R - R_{\mathrm{m}}$ is the displacement coordinate from the equilibrium geometry R_m, and D, γ, and a_i are parameters to be determined from a least-squares fit to the calculated *ab initio* CASSCF points. However, for the OH($^4\Sigma^-$) repulsive state, it proved sufficient to use the simpler screened-Coulomb form

$$V_{\mathrm{EHF}} = DR^{-1} \exp(-\gamma R) \tag{4}$$

with the parameters D and γ being determined in the same way as for eq 3.

The dynamical correlation is in turn represented by

$$V_{\mathrm{dc}} = -\sum_{n=6,8,10} C_n \chi_n(R) R^{-n} \tag{5}$$

where the damping functions χ_n assume the form[20]

$$\chi_n = [1 - \exp(-A_n R/\rho - B_{\mathrm{n}} R^2/\rho^2)]^n \tag{6}$$

In turn, A_n and B_n are auxiliary functions given by

$$A_n = \alpha_0 n^{-\alpha_1}$$

$$B_n = \beta_0 e^{-\beta_1 n} \tag{7}$$

where α_i and β_i are dimensionless parameters which have been determined from a fit[8] to the *ab initio* perturbation results for the $H_2(b^3\Sigma_u^+)$ interaction: $\alpha_0 = 25.9258$, $\alpha_1 = 1.1868$, $\beta_0 = 15.7381$, and $\beta_1 = 0.097\,29$. Moreover, $\rho = (R_{\mathrm{m}}/2 + 1.25R_0)$ is a scaling distance written in terms of the equilibrium geometry R_{m}, and $R_0 = 2(\langle r_{\mathrm{M}}^2\rangle^{1/2} + \langle r_{\mathrm{X}}^2\rangle^{1/2})$ is the Le Roy[18] parameter, which has been suggested to represent the smallest internuclear distance for which the asymptotic series of the dispersion energy is still a good representation of the damped series in eq 5. Note that $\langle r_{\mathrm{X}}^2\rangle(\langle r_{\mathrm{M}}^2\rangle)$ is the expectation value of the squared radii for the outermost electrons in atom X(M);[19] for a somewhat simpler parametrization in eqs 6 and 7, see ref 20. Finally, following Varandas,[4] we assume that the values of the C_8 and C_{10} dispersion coefficients can be estimated using the universal correlation

$$\frac{C_n}{C_6} = \kappa_n R_0^{a(n-6)/2} \tag{8}$$

where $\kappa_8 = 1$, $\kappa_{10} = 1.31$, and $a = 1.54$ are parameters.

To obtain the dispersion coefficients C_n in eq 5, we have adopted the following procedure. First, we subtract, for each grid point, the CASSCF energy value from the calculated total (CASPT2) energy, after removal of the asymptotic CASPT2 and CASSCF energies. We then fit (for $R > R_0$) the dynamical correlation energy so obtained from eq 5, while using eq 8 to estimate the C_8 and C_{10} dispersion coefficients.

3. Computational Details

To study the diatomic fragments in Table 1, we have performed both CASSCF and CASPT2 calculations. These calculations have encompassed a grid of 26 different internuclear distances (from 1.4 to 30 a_0). The points in the grid were not equally spaced and have been densely distributed in the neighborhood of the minimum of each diatomic. Although our first attempt to the dynamical correlation energy has been to use a configuration interaction approach including all single and double excitations from the full-valence CASSCF reference function, such CASSCF CISD calculations have proved too expensive for the diatomics involving the atoms C, N, and O. For consistency reasons discussed above, particularly having in mind that similar calculations should be carried out for the triatomic and tetraatomic species, such methodology has been replaced by the more economical CASPT2 one. To perform these CASPT2 calculations, the MOLCAS-3 package[21] has been employed.

Once the energies have been calculated, they have been fitted to eqs 3 and 5 using the least-squares method as mentioned in section 2. This involves a linear procedure for eq 5, and a mixed nonlinear−linear procedure for eqs 3 or 4. In the latter, the nonlinear parameters have been determined iteratively using the Levengerg−Marquardt[22] method until convergence was reached, the linear parameters being optimized at every iteration. This procedure consists of using a steepest descent method far from the minimum, while a continuous switch to the inverse Hessian method is employed as the minimum is approached.

In all CASSCF calculations, the active space has been the valence space. For the CASPT2 calculations, all but the 1s electrons have been correlated using the CASSCF wave function as the reference.[23]

3.1. Basis Sets. Since a major aim of this work has been the search for a reasonable accuracy/computational cost ratio, we have studied five different basis sets of increasing level of sophistication. Of these, we used the largest one as reference, and then compared the results obtained from it with triple-ζ, enlarged double-ζ, and double-ζ basis sets. Specifically, the basis sets employed in this work are (i) the cc-pVDZ 9s4p1d/[3s2p1d] for C, N, and O and 4s1p/[2s1p] for H basis set of Dunning *et al.*,[24] (ii) the D-95 9s5p1d/[4s2p1d] for C, N, and O and 4s2p/[2s1p] for H basis set of Dunning *et al.*,[25] (iii) the contracted ANO 10s6p3d/[7s6p3d] for C, N, and O and 7s3p/[4s3p] for H basis set of Pierloot *et al.*,[26] (iv) the cc-pVTZ 10s5p2d1f/[4s3p2d1f] for C, N, and O and 5s2p1d/[3s2p1d] for H basis set of Dunning *et al.*,[24] and (v) the contracted ANO 14s9p4d3f/[5s4p3d2f] for C, N, and O and 8s4p3d/[3s2p1d] for H basis set of Widmark *et al.*[27]

4. Results and Discussion

The results obtained for the electronic states of the diatomic molecules listed in Table 1 are summarized in Tables 2−9 for each basis set described in section 3. Tables 2 and 5 give the calculated values of the dissociation energy (D_{e}) and equilibrium geometry (R_{m}), which are also compared with the corresponding experimental values from reference 28.

As might be expected, Tables 2 and 5 show that the best results are obtained with the Widmark ANO [5s4p3d2f] basis set both for the dissociation energy and the equilibrium geometry

TABLE 2: Values for D_e and R_m Obtained for the Ground States of the Diatomic Molecules in Table 1

system	basis set	D_e^{CASSCF}[a]	D_e^{CASPT2}	D_e^{exp28}	R_m^{CASSCF}	R_m^{CASPT2}	$R_m^{(exp)\ 28}$
CH($X^2\Pi$)	D-95 dz	0.108 05	0.120 30	0.133 8	2.162	2.140	2.116
	cc-pVDZ	0.105 80	0.118 09		2.177	2.160	
	cc-pVTZ	0.108 54	0.126 72		2.152	2.116	
	ANO [7s6p3d]	0.108 77	0.122 70		2.147	2.120	
	ANO [5s4p3d2f]	0.108 94	0.128 28		2.149	2.116	
OH($X^2\Pi$)	D-95 dz	0.132 49	0.155 30	0.169 92	1.848	1.843	1.832
	cc-pVDZ	0.128 31	0.149 83		1.854	1.846	
	cc-pVTZ	0.133 84	0.162 72		1.834	1.825	
	ANO [7s6p3d]	0.134 73	0.160 40		1.833	1.825	
	ANO [5s4p3d2f]	0.135 09	0.165 93		1.831	1.821	
NO($X^2\Pi$)	D-95 dz	0.195 58	0.205 87	0.243 0	2.223	2.234	2.175
	cc-pVDZ	0.200 11	0.212 79		2.201	2.203	
	cc-pVTZ	0.206 89	0.227 79		2.190	2.184	
	ANO [7s6p3d]	0.203 75	0.215 65		2.193	2.192	
	ANO [5s4p3d2f]	0.207 32	0.235 20		2.188	2.174	
CN($X^2\Sigma$)	D-95 dz	0.256 19	0.254 86	0.289 7	2.259	2.265	2.214
	cc-pVDZ	0.260 09	0.258 58		2.258	2.258	
	cc-pVTZ	0.266 39	0.274 87		2.233	2.227	
	ANO [7s6p3d]	0.264 73	0.263 97		2.231	2.226	
	ANO [5s4p3d2f]	0.267 00	0.284 25		2.231	2.221	
NH($X^3\Sigma^-$)	D-95 dz	0.101 63	0.116 03	0.135 0	1.996	1.988	1.958
	cc-pVDZ	0.098 45	0.112 68		2.005	1.999	
	cc-pVTZ	0.102 57	0.123 65		1.986	1.971	
	ANO [7s6p3d]	0.103 15	0.119 86		1.983	1.971	
	ANO [5s4p3d2f]	0.103 39	0.126 35		1.984	1.967	
CO($X^1\Sigma$)	D-95 dz	0.386 93	0.378 51	0.412 7	2.172	2.178	2.276
	cc-pVDZ	0.392 58	0.383 75		2.158	2.161	
	cc-pVTZ	0.400 41	0.396 81		2.146	2.142	
	ANO [7s6p3d]	0.399 50	0.388 71		2.144	2.141	
	ANO [5s4p3d2f]	0.400 98	0.404 01		2.143	2.133	

[a] All quantities are in atomic units: energies in E_h, distances in a_0.

TABLE 3: Values of the Parameters in Equation 3 for the Ground States of the Diatomic Molecules in Table 1. Units as in Table 2

system	basis set	D	a_1	a_2	a_3	γ
CH($X^2\Pi$)	D-95 dz	0.233 64	2.527 57	1.866 03	0.592 58	2.040 37
	cc-pVDZ	0.230 31	2.519 21	1.828 61	0.565 10	2.033 37
	cc-pVTZ	0.233 53	2.530 76	1.898 03	0.619 21	2.042 85
	ANO [7s6p3d]	0.233 56	2.526 23	1.878 80	0.608 92	2.035 44
	ANO [5s4p3d2f]	0.234 15	2.531 45	1.894 62	0.614 90	2.042 67
OH($X^2\Pi$)	D-95 dz	0.244 82	3.154 54	3.034 75	1.399 00	2.587 15
	cc-pVDZ	0.237 55	3.181 68	3.118 49	1.433 64	2.620 41
	cc-pVTZ	0.245 48	3.225 28	3.282 27	1.614 80	2.643 98
	ANO [7s6p3d]	0.246 91	3.225 83	3.288 75	1.620 35	2.642 81
	ANO [5s4p3d2f]	0.247 40	3.227 90	3.288 41	1.623 95	2.643 75
NO($X^2\Pi$)	D-95 dz	0.434 72	3.724 29	4.043 56	1.570 66	3.304 91
	cc-pVDZ	0.440 46	3.731 27	4.058 20	1.600 38	3.292 52
	cc-pVTZ	0.452 98	3.726 76	4.135 34	1.679 91	3.271 09
	ANO [7s6p3d]	0.446 88	3.724 60	4.144 61	1.685 95	3.265 96
	ANO [5s4p3d2f]	0.453 53	3.739 05	4.175 63	1.699 99	3.277 39
CN($X^2\Sigma$)	D-95 dz	0.578 86	3.473 48	3.686 62	1.415 36	3.047 84
	cc-pVDZ	0.585 76	3.481 86	3.705 50	1.429 52	3.049 85
	cc-pVTZ	0.594 92	3.480 81	3.754 81	1.488 55	3.024 92
	ANO [7s6p3d]	0.590 61	3.428 68	3.757 69	1.491 81	3.023 45
	ANO [5s4p3d2f]	0.595 59	3.482 04	3.762 56	1.495 98	3.022 73
NH($X^3\Sigma^-$)	D-95 dz	0.202 81	3.125 42	3.022 68	1.240 03	2.616 64
	cc-pVDZ	0.197 38	3.151 88	3.081 02	1.262 66	2.642 11
	cc-pVTZ	0.203 70	3.169 31	3.193 63	1.370 63	2.659 47
	ANO [7s6p3d]	0.204 53	3.171 94	3.201 94	1.379 86	2.660 91
	ANO [5s4p3d2f]	0.205 11	3.174 50	3.208 47	1.380 05	2.664 24
CO($X^1\Sigma$)	D-95 dz	0.840 57	2.696 56	1.937 30	0.602 31	2.208 66
	cc-pVDZ	0.847 20	2.704 81	1.970 97	0.635 95	2.217 67
	cc-pVTZ	0.859 28	2.807 64	2.274 23	0.813 42	2.301 87
	ANO [7s6p3d]	0.856 68	2.782 37	2.210 88	0.782 18	2.276 62
	ANO [5s4p3d2f]	0.859 15	2.802 58	2.262 53	0.811 10	2.295 31

for all diatomic fragments except for CO($^1\Sigma$). For the equilibrium geometry, the difference between theory (at the CASPT2 level[27]) and experiment is in all cases but CO($X^1\Sigma$) smaller than 0.02 a_0. On the other hand, it is well-known that the CASPT2 method systematically underestimates all bond energies by $(5 \times 10^{-3})-(1 \times 10^{-2})$ E_h,[29] which explains the observed discrepancies between the CASPT2 values in Tables 2 and 5 and the experimental results. This may also explain the larger discrepancies found for NO($X^2\Pi$) and CO($X^1\Sigma$), since in these cases three electron pairs are formed in the bonding process.

Another important observation from Tables 2 and 5 is that basis set effects are more marked in the CASPT2 calculations

TABLE 4: Values of the Parameters in Equation 5 for the Ground States of the Diatomic Molecules in Table 1. Units as in Table 2

system	basis set	C_6	$C_8 \times 10^{-2}$	$C_{10} \times 10^{-3}$
CH($X^2\Pi$)	D-95 dz	10.344	2.4003	6.2938
	cc-pVDZ	10.592	2.4579	6.4448
	cc-pVTZ	16.183	3.7553	9.8466
	ANO [7s6p3d]	12.339	2.8632	7.5076
	ANO [5s4p3d2f]	17.017	3.9487	10.354
OH($X^2\Pi$)	D-95 dz	7.8001	1.4013	2.8446
	cc-pVDZ	7.4241	1.3337	2.7075
	cc-pVTZ	9.9273	1.7834	3.6204
	ANO [7s6p3d]	9.0502	1.6259	3.3005
	ANO [5s4p3d2f]	10.722	1.9261	3.9099
NO($X^2\Pi$)	D-95 dz	4.3280	0.74382	1.4445
	cc-pVDZ	4.8672	0.83650	1.6245
	cc-pVTZ	8.9812	1.5436	2.9977
	ANO [7s6p3d]	6.3136	1.0851	2.1073
	ANO [5s4p3d2f]	12.051	2.0712	4.0224
CN($X^2\Sigma$)	D-95 dz	7.2765	1.6263	4.1073
	cc-pVDZ	7.3203	1.6361	4.1320
	cc-pVTZ	9.1245	2.0393	5.1504
	ANO [7s6p3d]	11.271	2.5191	6.3621
	ANO [5s4p3d2f]	16.914	3.7803	9.5474
NH($X^3\Sigma^-$)	D-95 dz	7.1693	1.4381	3.2587
	cc-pVDZ	7.3187	1.4681	3.3277
	cc-pVTZ	10.818	2.1700	4.9187
	ANO [7s6p3d]	8.7474	1.7547	3.9773
	ANO [5s4p3d2f]	11.820	2.3710	5.3743
CO($X^1\Sigma$)	D-95 dz	13.414	2.7054	6.1656
	cc-pVDZ	11.505	2.3204	5.2883
	cc-pVTZ	12.021	2.4244	5.5253
	ANO [7s6p3d]	24.284	4.8976	11.1618
	ANO [5s4p3d2f]	18.299	3.6906	8.4109

than in the CASSCF ones. This is due to the fact that the dynamical correlation obtained from the CASPT2 calculations is more sensitive to the size of the basis set than the nondynamical correlation (this is the only correlation obtained at the CASSCF level).

Tables 3 and 6 report the results obtained from the fitting of the *ab initio* CASSCF energies to eq 3 and to eq 4 for OH ($a^4\Sigma^-$). It is seen that the values of the linear parameters a_i and the nonlinear one γ are very similar for all basis sets employed, which reflects the previously mentioned fact concerning the CASSCF calculations. Nevertheless we can appreciate a slight difference in the parameters obtained for the double zeta basis sets (D-95 and cc-pVDZ) and those obtained with the larger basis sets (triple-ζ cc-pVTZ and ANO [5s4p3d2f]). Finally, we note that the values determined with the cc-pVDZ and ANO [7s6p3d] basis sets and those obtained with the largest basis set employed ([5s4p3d2f]) are very close in all cases except in that of the OH($a^4\Sigma^-$) repulsive state.

Concerning the dynamical correlation, Tables 4 and 7 give the values obtained for the C_n coefficients in eq 5 following the procedure described in the section 3. First, we observe a more marked influence of the basis set on the reported quantities. Then, we observe from Tables 4 and 7 that the value of the C_n dispersion coefficients increase with increasing basis set size, which may be attributed to a better reproduction of the dynamical correlation with basis set quality; this leads to a larger difference between the CASSCF (nearly invariant in all basis sets) and the CASPT2 energies, and hence implies higher values of the C_n dispersion coefficients. Thus, we will assume that the most reliable C_n values are the largest ones calculated for each diatomic. This corresponds also to the largest basis set [5s4p3d2f] in all cases except in that of CO($X^1\Sigma^+$). Again, this is probably due to the deficiencies of the CASPT2 method in representing this state. In Table 8, we compare our best values (in the sense implied above) obtained for the C_6 coefficient with those available in the literature. Except for the OH dispersion coefficient C_6, all others have been calculated as the geometric average of the dispersion coefficients of the associated homonuclear interactions.[30] In turn, the C_6 OH coefficient has been determined using perturbation theory by Varandas and Voro-

TABLE 5: Values of D_e and R_e in the Calculations for the Excited States of the Diatomic Molecules in Table 1. Units as in Table 2

system	basis set	D_e^{CASSCF}	D_e^{CASPT2}	$D^{exp\ 28}$	R_m^{CASSCF}	R_m^{CASPT2}	$R_m^{(exp)\ 28}$
CH($a^4\Sigma^-$)	D-95 dz	0.101 219	0.105 953		2.067	2.064	2.050
	cc-pVDZ	0.097 527	0.102 229		2.083	2.086	
	cc-pVTZ	0.100 075	0.107 776		2.061	2.050	
	ANO [7s6p3d]	0.999 830	0.104 665		2.059	2.056	
	ANO [5s4p3d2f]	0.100 282	0.108 830		2.061	2.053	
CO($a^3\Pi$)	D-95 dz	0.159 627	0.170 407		2.322	2.331	2.279
	cc-pVDZ	0.160 897	0.171 044		2.310	2.316	
	cc-pVTZ	0.167 789	0.184 266		2.296	2.294	
	ANO [7s6p3d]	0.166 873	0.177 090		2.292	2.293	
	ANO [5s4p3d2f]	0.168 826	0.192 098		2.290	2.280	

TABLE 6: Values of the Parameters in Equations 3 and 4 for the Excited States of the Diatomic Molecules in Table 1. Units as in Table 2

system	basis set	D	a_1	a_2	a_3	γ
CH($a^4\Sigma^-$)	D-95 dz	0.209 242	3.668 29	4.645 14	2.289 56	3.099 52
	cc-pVDZ	0.203 158	3.721 93	4.758 68	2.335 59	3.153 78
	cc-pVTZ	0.206 279	3.712 68	4.809 07	2.427 87	3.134 87
	ANO [7s6p3d]	0.205 901	3.715 45	4.811 98	2.429 27	3.137 37
	ANO [5s4p3d2f]	0.206 669	3.713 49	4.811 25	2.428 28	3.135 57
OH($a^4\Sigma^-$)	D-95 dz	1.979 59	nr[a]	nr	nr	1.010 73
	CC-ppVDZ	1.586 13	nr	nr	nr	0.950 40
	cc-pVTZ	1.285 60	nr	nr	nr	0.883 68
	ANO [7s6p3d]	0.991 42	nr	nr	nr	0.793 95
	ANO [5s4p3d2f]	0.984 67	nr	nr	nr	0.787 53
CO($a^3\Pi$)	D-95 dz	0.370 656	3.672 34	3.934 95	1.453 69	3.365 16
	cc-pVDZ	0.371 674	3.680 38	3.969 67	1.486 36	3.360 94
	cc-pVTZ	0.385 218	3.666 09	3.981 03	1.510 92	3.324 02
	ANO [7s6p3d]	0.382 536	3.638 16	3.899 11	1.460 24	3.283 03
	ANO [5s4p3d2f]	0.386 669	3.668 14	3.991 33	1.516 32	3.318 74

[a] nr = not relevant. See the text.

TABLE 7: Values of the Parameters in Equation 5 for the Excited States of the Diatomic Molecules in Table 1. Units as in Table 2

system	basis set	C_6	$C_8 \times 10^{-2}$	$C_{10} \times 10^{-3}$
CH($a^4\Sigma^-$)	D-95 dz	4.058 20	0.941 68	2.469 2
	cc-pVDZ	4.240 67	0.984 04	2.580 3
	cc-pVTZ	7.339 23	1.703 05	4.465 7
	ANO [7s6p3d]	4.816 34	1.117 62	2.930 5
	ANO [5s4p3d2f]	8.010 64	1.858 85	4.874 1
OH($a^4\Sigma^-$)	D-95 dz	2.238 52	0.402 14	0.816 32
	cc-pVDZ	2.706 11	0.486 14	0.986 84
	cc-pVTZ	2.580 53	0.463 58	0.941 04
	ANO [7s6p3d]	2.256 52	0.405 37	0.822 89
	ANO [5s4p3d2f]	2.470 97	0.443 89	0.901 09
CO($a^3\Pi$)	D-95 dz	6.363 35	1.283 37	2.924 81
	cc-pVDZ	6.362 63	1.283 23	2.924 48
	cc-pVTZ	11.752 4	2.370 26	5.401 82
	ANO [7s6p3d]	8.275 54	1.669 03	3.803 72
	ANO [5s4p3d2f]	16.106 6	3.248 41	7.403 14

TABLE 8: Comparison of the Fitted C_6 Values with Those Available in the Literature. Units as in Table 2

system	C_6	C_6^{ref}
CH($X^2\Pi$)	17.017	16.11
OH($X^2\Pi$)	10.722	11.47[31]
NO($X^2\Pi$)	12.051	18.70[36]
CN($X^2\Sigma$)	16.914	30.17
NH($X^3\Sigma^-$)	11.820	12.17
CO($X^1\Sigma$)	18.299	24.80[36]
CH($a^4\Sigma^-$)	8.0106	16.11
OH($a^4\Sigma^-$)	2.4710	13.26[31]
CO($a^3\Pi$)	16.107	24.80[31]

TABLE 9: Values for the Parameters in Equations 3 and 4 for the States of the Diatomic Molecules in Table 1. Units as in Table 2. The C_n Dispersion Coefficients have been Fixed at Their Best Semiempirical Values

system	D(au)	a_1	a_2	a_3	γ
CH($X^2\Pi$)	0.234 15	2.517 13	1.976 39	0.717 44	2.021 30
OH($X^2\Pi$)	0.271 00	3.151 55	3.245 70	1.759 50	2.524 17
NO($X^2\Pi$)	0.453 53	3.292 38	2.915 34	0.984 60	2.791 33
CN($X^2\Sigma$)	0.595 59	3.349 44	3.376 71	1.270 46	2.864 28
NH($X^3\Sigma^-$)	0.205 11	3.014 82	2.892 43	1.258 78	2.479 05
CO($X^1\Sigma$)	0.808 92	2.332 74	1.062 22	0.262 22	1.839 13
CH($a^4\Sigma^-$)	0.196 02	3.524 55	4.181 29	1.971 25	2.914 56
OH($a^4\Sigma^-$)	1.369 82	nr	nr	nr	1.030 95
CO($a^3\Pi$)	0.386 67	3.350 54	3.103 35	1.035 73	2.884 84

nin.[31] For all diatomic ground states involving a H atom, the agreement is good. It is only moderate or even poor for the interactions in which both atoms are different from H, which is probably due to the less accurate description of such systems in the CASPT2 approach; note that more than one electron pair can now be formed. Moreover, very poor agreement is found for the Σ^- excited states. This may in turn be explained due to the fact that the Σ^- configurations can only be formed by using the p_x and p_y orbitals of the heavy atom (z being the axis of the diatomic molecule). This reduces drastically the number of configuration state functions obtained within the active space and also within the allowed CSFs for the CASPT2 calculation, leading to results for the energy that cannot be considered to have a level of accuracy similar to that reached for the other states.

An alternative approach to the parameters in eq 3 consists of using the best available semiempirical values for the C_n dispersion coefficients. In this case, the dynamical correlation in eq 5 is set *a priori* from those dispersion coefficients and then subtracted from the calculated CASPT2 energies to yield effective EHF energies; these are next used in a way similar to that described above for the true CASSCF points to obtain the parameters in eq 3. This inverse procedure has been used to obtain the coefficients a_i and γ of eq 3 for the largest basis set (ANO [5s4p3d2f]). The results are shown in Table 9. The numerical values obtained using this procedure are in very good agreement with the previously obtained ones. As expected, the larger differences are found when the experimental C_6 coefficient and the calculated one are not in good agreement.

Finally, to calibrate the results obtained with the DMBE method for the diatomic systems, we show in Figures 1−3 a comparison of the results obtained with the ANO [5s4p3d2f] basis set with the available accurate RKR spectroscopic data[32−34] employing the C_n dispersion coefficients obtained from our fit,

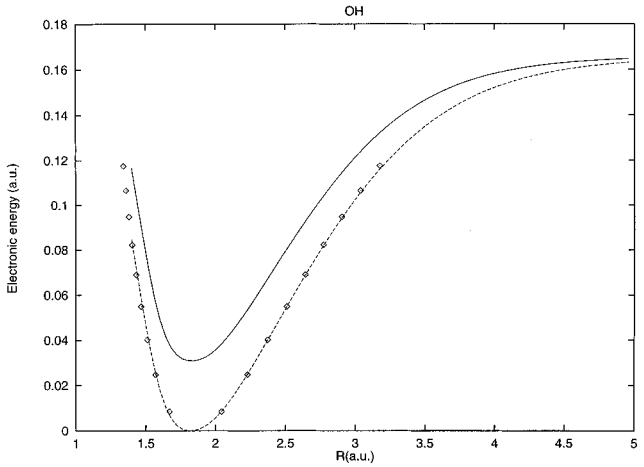

Figure 1. OH($X^2\Pi$) potential. Comparison with RKR data:[32] (−) EHF, (− −) EHF+dc, (◇) RKR data.

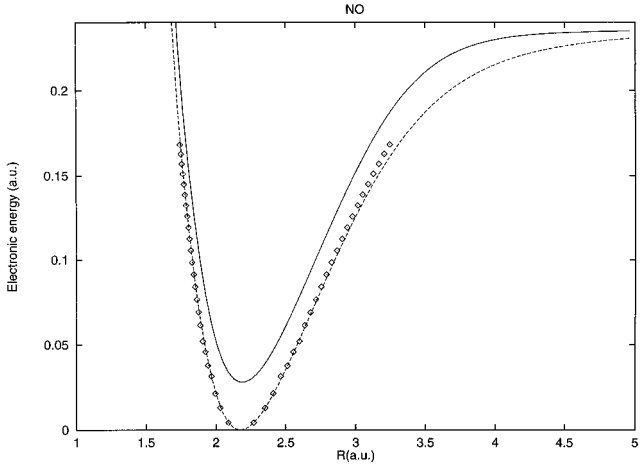

Figure 2. NO($X^2\Pi$) potential. Comparison with RKR data:[33] (−) EHF, (− −) EHF+dc, (◇) RKR data.

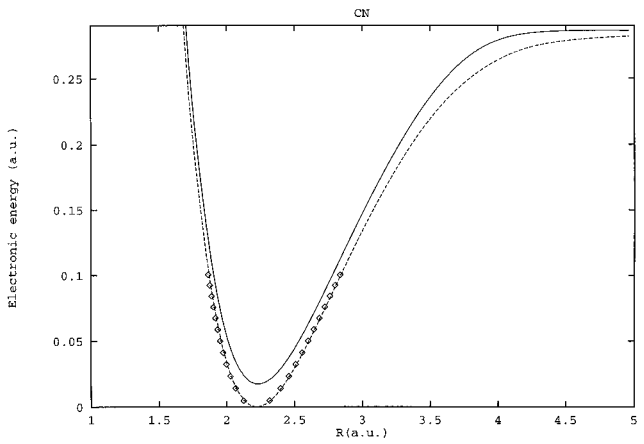

Figure 3. CN($X^2\Pi$) potential. Comparison with RKR data:[34] (−) EHF, (− −) EHF+dc, (◇) RKR data.

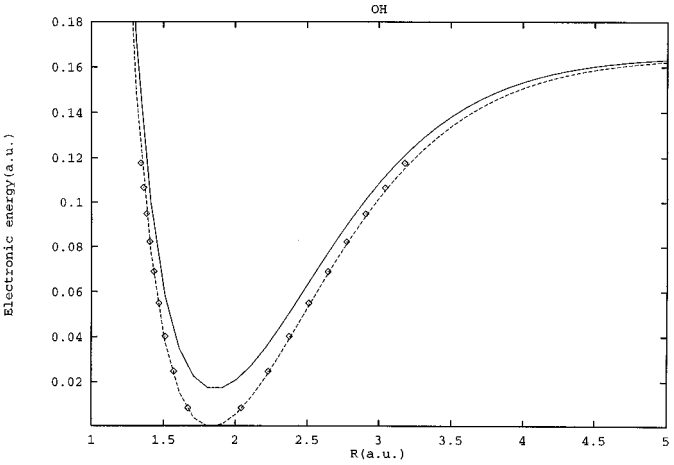

Figure 4. OH($X^2\Pi$) potential with fixed semiempirical values for C_n. Comparison with RKR data:[32] (−) EHF, (− −) EHF+dc, (◊) RKR data.

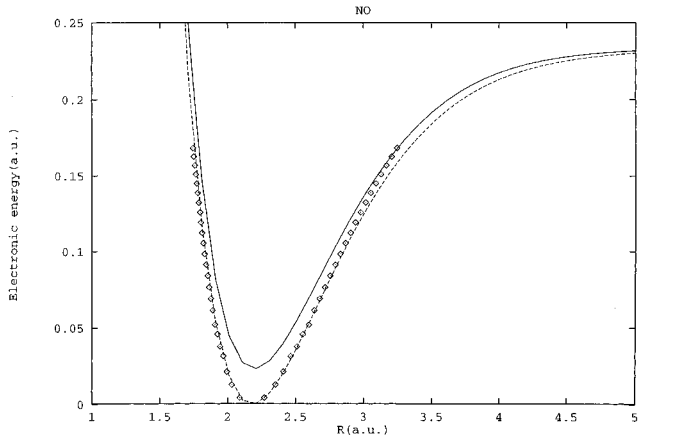

Figure 5. NO($X^2\Pi$) potential with fixed semiempirical values for C_n. Comparison with RKR data:[33] (−) EHF, (− −) EHF+dc, (◊) RKR data.

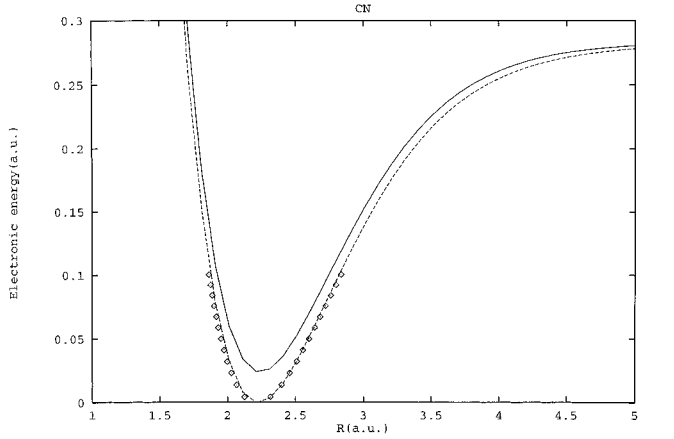

Figure 6. CN($X^2\Sigma$) potential with fixed semiempirical values for C_n. Comparison with RKR data:[34] (−) EHF, (− −) EHF+dc, (◊) RKR data.

and in Figures 4−6 we show the results obtained with the alternative approach which keeps the best available semiempirical values for the C_n dispersion coefficients. Clearly, there is very good agreement for all systems. The slight difference we can appreciate (especially for NO($X^2\Pi$)) is partly due to the difference between the dissociation energies already reported in Table 2. Such a problem can be overcome by adding a semiempirical correction. This correction[35] (named SEC from the initials of scaling external correlation) is based on the assumption that the *ab initio* dynamical correlation is underestimated by the same fraction over the whole range of internuclear distances. Thus, to obtain a realistic description of the dynamical correlation, one just requires to scale it in such a way that the calculated total potential energy (obtained by adding the scaled dynamical correlation to the *ab initio* extended Hartree−Fock energy) reproduces exactly the known experimental dissociation energy.

5. Conclusions

Five different basis sets have been employed to obtain the potential curves of six diatomics (involving nine electronic states) relevant for building the CHNO PES according to the DMBE strategy. Both the EHF and dynamical correlation parts of the calculated energies have been modelled analytically using forms from the realistic EHFACE2 model. The relevant numerical coefficients have been tabulated for the nine studied electronic states. Large differences have been observed between the results obtained from the two smaller basis sets and the biggest one both for the EHF and dynamical correlation energies. Within the larger basis sets, it is worth noting that almost the same result is obtained using the cc-pVTZ [4s3p2d1f] and the ANO [5s4p3d2f] basis sets, while the computational effort required for the first is significantly smaller. Regarding the dispersion coefficients C_n, we have found a reasonable agreement with other theoretical results available in the literature. For OH($X^2\Pi$), the agreement found with the accurate value of Varandas *et al*.[31] is particularly good. In summary, the present studies suggest that the cc-pVTZ [4s3p2s1f] basis set is probably the most suited to perform the *ab initio* calculations of the triatomic and tetraatomic systems necessary for the study of the title potential energy surface. In fact, we have shown that it gives results very close to those obtained by using the largest basis set employed (ANO [5s4p3d2f]) in the present work, while keeping the computational cost at an affordable level.

Acknowledgment. This work has been carried out under the auspices of the EC grants (Contracts CHRXCT 94-0436 and ERBCHBG CT 93-0337). A scholarship of the Junta Nacional de Investigação Científica e Tecnológica, under programme PRAXIS XXI, is also gratefully acknowledged by one of us (P.E.A.).

References and Notes

(1) Murrell, J. N.; Carter, S.; Farantos, S. C.; Huxley, P.; Varandas, A. J. C. *Molecular Potential Energy Functions*; Wiley: Chichester, 1984.
(2) Sathyamurthy, N. *Comput. Phys. Rep.* **1985**, *3*, 1.
(3) Truhlar, D. G.; Steckler, R.; Gordon, M. S. *Chem. Rev.* **1987**, *87*, 217.
(4) Varandas, A. J. C. *Adv. Chem. Phys.* **1988**, *74*, 255.
(5) Buckingham, A. D.; Fowler, P. W.; Hutson, J. M. *Chem. Rev.* **1988**, *88*, 963.
(6) Schatz, G. C. *Rev. Mod. Phys.* **1989**, *61*, 669.
(7) Varandas, A. J. C. *Mol. Phys.* **1984**, *53*, 1303.
(8) Varandas, A. J. C. *J. Mol. Struct. (THEOCHEM)* **1985**, *120*, 401.
(9) Varandas, A. J. C.; Brandão, J.; Quintales, L. A. M. *J. Phys. Chem.* **1988**, *92*, 3732.
(10) Pastrana, M. R.; Quintales, L. A. M.; Brandão, J.; Varandas, A. J. C. *J. Phys. Chem.* **1990**, *94*, 8073.
(11) Varandas, A. J. C.; Voronin, A. I. *Mol. Phys.* **1995**, *95*, 497.
(12) Varandas, A. J. C.; Pais, A. A. C. C. *Mol. Phys.* **1988**, *65*, 843.
(13) Varandas, A. J. C. *Int. J. Quantum Chem.* **1987**, *32*, 563.
(14) Varandas, A. J. C.; Pais, A. A. C. C. *Theoretical and Computational Models for Organic Chemistry*; Formosinho, S. J., Czismadia, I. G., Arnaut, L. G., Eds.; Kluwer: Dordrecht, 1991; p 55.
(15) Varandas, A. J. C.; Yu, H. G. *Double Many-Body Expansion Potential Energy Surface for Ground-State* HO_3. In press.
(16) Anderson, K.; Malmqvist, P. Å.; Roos, B. O.; Sadlej, A. J.; Wolinski, K. *J. Phys. Chem.* **1990**, *94*, 5483.
(17) Varandas, A. J. C.; Silva, J. D. *J. Chem. Soc., Faraday Trans. 2* **1992**, *88*, 941.

(18) Le Roy, R. J. *Spec. Period Rep. Chem. Soc. Mol. Spectrosc.* **1973**, *1*, 113.
(19) Desclaux, J. P. *At. Data Nucl. Data Tables* **1973**, *12*, 311.
(20) Varandas, A. J. C. *Mol. Phys.* **1987**, *60*, 527.
(21) Anderson, K.; Blomberg, M. R. A.; Fülscher, M. P.; Kellö, V.; Lindh, R.; Malmqvist, P.-Å.; Noga, J.; Olsen, J.; Roos, B. O.; Sadlej, A. J.; Siegbahn, P. E. M.; Urban, M.; Widmark; P.-O. *MOLCAS*, Version 3; University of Lund: Sweden, 1994.
(22) Marquardt, D. W. *J. Soc. for Ind. Appl. Math.* **1963**, *11*, 431.
(23) The *ab initio* energies are available upon request from the authors.
(24) Dunning, T. H., Jr. *J. Chem. Phys.* **1993**, *99*, 9790.
(25) Dunning, T. H., Jr.; Hay, P. J. *Modern Theoretical Chemistry*; Schaefer, H. F., Ed.; Plenum: New York, 1977; Vol. 3 (Methods of Electronic Structure Theory), p 1.
(26) Pierloot, K.; Dumez, B.; Widmark, P. O.; Roos, B. O. *Theor. Chim. Acta* **1995**, *90*, 87.
(27) Widmark, P. O.; Malmqvist, P. Å.; Roos, B. O. *Theor. Chim. Acta* **1990**, *77*, 291.
(28) Huber, K. P.; Herzberg, G. *Molecular Spectra and Molecular Structure. IV. Constants of Diatomic Molecules*; van Nostrand: New York, 1979.
(29) Anderson, K.; Roos, B. O. *Int. J. Quantum Chem.* **1993**, *45*, 591.
(30) Staemmler, V.; Jaquet, R. *Chem. Phys.* **1985**, *92*, 141.
(31) Varandas, A. J. C.; Voronin, A. I. *Chem. Phys.* **1995**, *194*, 91.
(32) Fallon, R. J.; Tobias, I.; Vanderslice, J. T. *J. Chem. Phys.* **1961**, *34*, 167.
(33) Vanderslice, J. T. *J. Chem. Phys.* **1962**, *37*, 384.
(34) Prasad, C. V. V.; Bernath, P. F. *J. Mol. Spectrosc.* **1992**, *156*, 327.
(35) Varandas, A. J. C. *J. Chem. Phys.* **1989**, *90*, 4379.
(36) Varandas, A. J. C.; Silva, J. D. *J. Chem. Soc., Faraday Trans. 2* **1986**, *82*, 593.